Journal of CO2 Utilization 69 (2023) 102399

Contents lists available at ScienceDirect

Journal of CO2 Utilization

journal homepage: www.elsevier.com/locate/jcou

A newly isolated alkaliphilic cyanobacterium for biomass production with direct air CO_2 capture

Song Gao [a,*], Kyle Pittman [a], Scott Edmundson [a], Michael Huesemann [a], Mattias Greer [a], William Louie [a], Peter Chen [a], David Nobles [b], John Benemann [c], Braden Crowe [c]

[a] Pacific Northwest National Laboratory, Marine and Coastal Research Laboratory, 1529W Sequim Bay Rd, Sequim, WA 98382, USA
[b] University of Texas at Austin, UTEX Culture Collection of Algae, 205W. 24th Street, Stop A6700, Austin, TX 78712, USA
[c] MicroBio Engineering Inc., PO Box 15821, San Luis Obispo, CA 93406, USA

ARTICLE INFO

Keywords:
Alkaliphilic cyanobacteria
Biomass
Raceway pond
Direct air capture

ABSTRACT

Large-scale microalgal biomass production usually relies on concentrated CO_2 as the carbon source which is a major logistical and economic challenge because of the required infrastructure and geospatial constraints of siting large algal production facilities close to concentrated CO_2 sources. By taking advantage of enhanced CO_2 mass transfer within alkaline media due to the reaction between CO_2 and OH^-, carbon can be directly captured from the ambient air and used by the algae. Achieving such goal requires algal strains that can grow fast under alkaline conditions. In this study, a newly isolated alkaliphilic cyanobacterial strain *Cyanobacterium* sp. PNNL-SSL1 was characterized for its temperature, pH, and salinity tolerance. The result shows that PNNL-SSL1 could sustain grow at pH above 11.2 but exhibited the highest growth rates at pH below 10.5. The strain is a warm season strain and grows the best at 10 PSU (practical salinity unit). The strain was then evaluated in indoor climate simulation ponds under outdoor-relevant pond cultivation conditions with carbon supplied only through direct air CO_2 capture at the culture surface. Two batch culture runs, at slightly different initial pH, exhibited average biomass productivity of 15.2 g m^{-2} day^{-1} on ash-free dry weight basis. CO_2 was directly captured from the air at an average rate of 21.6 g CO_2 m^{-2} day^{-1} (78.8 tons ha^{-1} yr^{-1}), contributing 74% of the carbon fixed in the biomass. The results demonstrated that PNNL-SSL1 is a promising strain for biomass production using air CO_2 as the carbon source.

1. Introduction

Increasing population and industrialization have contributed to the massive energy and food/feed demands globally. The current fossil-fuel-dominated economy has led to increasing concentrations of atmospheric CO_2 and other greenhouse gases, placing the world under the threat of climate change [1,2]. In the interest of reducing the energy dependency on fossil fuels, developing alternative sustainable energy sources such as biofuels have attracted substantial research efforts [3,4]. Microalgal biomass has been investigated as an alternative source of biofuels due to its unique features, including fast growth rates, high lipid content, and being non-competitive with arable resources [5,6].

Microalgal biofuels are limited due to high production costs, with CO_2 supply and delivery being one of the significant cost drivers. In open paddlewheel-driven raceway ponds, a commonly used system for microalgae cultivation, the culture is in contact with air. Atmospheric CO_2 diffuses across the gas-liquid interface and enters the culture medium at a rate and direction dependent on the driving force for mass transfer. Air-CO_2 is first dissolved to form CO_2(aq), which reacts to form carbonic acid and rapidly equilibrates via the bicarbonate - carbonate buffer system (Eq. 1). In rapidly growing cultures, dissolved carbonic acid and bicarbonate are utilized by the algal cells for photosynthesis at a high rate. However, the net CO_2 in-gassing rate is relatively slow due to the slow reaction that forms carbonic acid, resulting in carbon depletion and growth inhibition. To restore this essential element in the culture medium, concentrated CO_2 is commonly transported to the cultivation site and used to improve the in-gassing driving force, which increases delivery cost and storage challenges [7,8].

$$CO_{2(aq)} + H_2O \rightleftharpoons H_2CO_3 \rightleftharpoons H^+ + HCO_3^- \rightleftharpoons CO_3^{2-} + H^+ \quad (1)$$

Compared to media at low alkalinity, media at high alkalinity can store a much larger amount of carbon due to the bicarbonate - carbonate

* Correspondence to: Pacific Northwest National Laboratory, 1529W Sequim Bay Rd., Sequim, WA 98382, USA.
E-mail address: Song.Gao@pnnl.gov (S. Gao).

https://doi.org/10.1016/j.jcou.2023.102399
Received 4 October 2022; Received in revised form 3 January 2023; Accepted 8 January 2023
Available online 19 January 2023

buffer system. To make use of such property, researchers proposed a bicarbonate-based cultivation system that allows carbon to be captured more efficiently and transported more easily in liquid form for algae growth [9,10]. Because of the carbonate buffering capability, pH of the alkaline medium is usually maintained at a higher level than in low alkalinity medium. In a high pH range, reaction between hydroxide ions and CO_2(aq) becomes the dominant reaction to produce bicarbonate (Eq. 2). Consequently, CO_2, even at a low concentration, is transferred across the gas-liquid interface at a significantly higher rate in the alkaline media than in low-alkalinity media. Recent studies have explored the possibility of growing microalgae with atmospheric CO_2 to fully exploit the enhanced CO_2 mass transfer rate. For instance, Ataeian et al. [11] demonstrated biomass production in an indoor tubular photobioreactor at pH up to 11.2, and the spent medium at high pH was sparged with air for 7 days to capture CO_2. For open systems such as raceway ponds, cultures are in direct contact with the air, and air-CO_2 can be captured without a separate carbonation/sparging unit. While some studies showed that biomass production could be supported solely by capturing CO_2 directly from the air [12], others suggested that additional mixing or carbonation station is a necessity for achieving sufficient carbon recharge [13,14].

$$CO_2 + OH^- \rightleftharpoons HCO_3^- \quad (2)$$

Regardless of the somewhat inconsistency in previous studies, to take advantage of the chemically enhanced CO_2 mass transfer, it is clear that the culture pH needs be kept as high as possible, as the enhancement effect of Eq. 2 is directly related to hydroxide ion concentration, i.e., pH [15,16]. However, most microalgal species recommended for biofuels production grow the best at near-neutral pH, and elevated pH beyond the optimal range significantly lowers the biomass productivity [17-19]. As a result of reduced biomass productivity, the cost of biomass, hence the cost of biofuels, can be increased substantially, making biofuel commercialization more challenging [7,20]. Therefore, it is critical to identify microalgal strains that can grow rapidly in alkaline conditions.

In the present study, *Cyanobacterium* sp. PNNL-SSL1, an alkaliphilic cyanobacterial strain, was isolated from Soap Lake, Washington, U.S., a naturally alkaline environment. The temperature, pH and salinity tolerance profiles of the strain were determined. To estimate its potential for biomass production with direct air CO_2 capture, PNNL-SSL1 was grown in duplicated indoor raceway ponds with air-CO_2 as the only external source for carbon. The areal biomass productivity obtained from the raceway experiment, where light and water temperature conditions for an outdoor pond culture were simulated, indicated that PNNL-SSL1 is a promising strain for biomass production that can rely on atmospherically derived CO_2.

2. Materials and methods

2.1. Strain isolation and identification

Surface water samples were collected from Soap Lake, Washington, U.S.A (47°23'36" N − 119°29'05" W). Sterile petri dishes, containing BG-11 [21] medium modified by adding 100 mM sodium bicarbonate and 1% (w/v) agar, were used to initiate isolation of individual agal colonies by streaking 100 µL of the collected water samples across the surface of the agar plate with a sterile microbiological transfer loop. Streaked plates were incubated under white (3000 K) LED light at a surface irradiance of ca. 800 µmol m^{-2} s^{-1} (LI-COR 190 R quantum sensor, LI-COR Inc. Lincoln, Nebraska) on a 12:12 photoperiod. Development of visually distinct algal colonies took approximately 7 days. After this incubation period, individual colonies were lifted and re-streaked using sterile technique onto sterile agar plates using the previously described modified BG-11 medium. The inoculated plates were maintained at 20 °C. As new colonies were formed, this streaking method was applied again. The process was repeated until unialgal colonies were obtained (i.e., single morphology, color, etc.).

Total DNA was extracted from the purified sample as previously described [22]. For PCR, Platinum Taq Polymerase (Thermo Fisher Scientific, Waltham, MA USA) was used with primers designed to amplify 23 s rDNA [23]. PCR products were purified using the GeneJET PCR Purification Kit (Thermo Fisher Scientific, Waltham, MA USA). Sanger sequencing was performed at the University of Texas at Austin Genomics Core Facility using Applied Biosystems 3730/3730XL DNA Analyzers and BigDye Terminator v3.1.

A consensus sequence for a partial 23 s rDNA sequence was obtained from 3 bidirectional sequence pairs. Similar sequences for phylogenetic tree construction were identified from the NCBI nucleotide database using BLAST [24]. A multiple alignment was created using the Clustal Omega plugin in Geneious Prime® 2022.2.2 (https://www.geneious.com). The multiple alignment was manually edited to remove gaps and poorly aligned regions. Phylogenetic analyses were performed with Bayesian Inference (BI), Maximum Likelihood (ML), and Neighbor Joining (NJ) using the Mr. Bayes, RAxML, and Geneious Treebuilder plugins from Geneious Prime® 2022.2.2 (https://www.geneious.com), respectively. BI was conducted using the GTR substitution model with gamma rate variation, a chain length of 1100,000, and a burn-in length of 100,000. ML was conducted using the GTR CAT model with 1000 bootstrap replicates. NJ was conducted using the Tamura-Nei genetic distance model with 10,000 bootstrap replicates.

2.2. Culture medium

The medium used for growing the strain was a modified BG-11 containing the followings in g L^{-1}: 0.75 $NaNO_3$, 0.04 $K_2HPO_4{\cdot}3\ H_2O$, 0.075 $MgSO_4{\cdot}7\ H_2O$, 0.027 $CaCl_2{\cdot}2\ H_2O$, 0.006 $(NH_4)_5[Fe(C_6H_4O_7)_2]$, 8.45 NaCl, 0.92 KCl, 4.2 $NaHCO_3$, 7.42 Na_2CO_3, 0.01 $Na_2EDTA{\cdot}2\ H_2O$, 0.029 H_3BO_3, 0.018 $MnCl_2{\cdot}4\ H_2O$, 0.0022 $CuSO_4{\cdot}5\ H_2O$, 0.0039 $Na_2MoO_4{\cdot}2\ H_2O$, 0.0005 $Co(NO_3)_2{\cdot}6\ H_2O$. The modified BG-11 medium had a final salinity of ca. 18 PSU (practical salinity unit) and a total carbonate alkalinity of 190 meq L^{-1}. Due to the higher salinity and inorganic carbon concentration than standard BG-11, the pH of this medium, once equilibrated with air, was approximately 9.9.

2.3. Determination of temperature, pH and salinity tolerance profiles

The temperature tolerance profile of the strain was determined by measuring the maximum specific growth rate as a function of temperature. The experiments were carried out on a customized shaker table (100 RPM mixing speed) that allows incubation of eight cultures in Erlenmeyer flask with a working volume of 75 ML over a temperature gradient of 3–45 °C [25]. The shaker table was operated at 100 rotations per minute (rpm) for mixing the cultures. Neutral white (4000 K) LED panels were used to provide light at ca. 450 µmol photons m^{-2} s^{-1}, measured by a LI-COR 190 R quantum senor, at the culture surface within the flask on a 12 hr:12 hr (light:dark) photoperiod. Cultures were sparged with sterile-filtered ambient air, containing 410 ppm CO_2, at a rate of 100 ML min^{-1} to keep the pH similar across all the cultures (9.7 ± 0.3).

After the inoculation, the cultures were grown for 48 h to acclimate to their respective temperatures. Following acclimation, the specific growth rates were obtained by measuring optical density via spectrophotometry at 750 nm (OD_{750}). Every day at the beginning of the photoperiod, the cultures were diluted to an OD_{750} of ca. 0.1 with fresh medium. OD_{750} was measured every three hours. The daily specific growth rate was calculated by taking the slope of the natural log transformed OD_{750} over time. The cultures were shallow (i.e., 2 cm) and remained at a low cell density ($OD_{750} < 0.3$), which ensures that the calculated specific growth rate represents the maximum specific growth rate at saturating light intensity. The trials were repeated until consistent specific growth rate at each temperature were observed.

To determine the pH tolerance profile, the maximum specific growth rate of the strain was measured as a function of pH, following the same

operation described in the last paragraph. Instead of varying temperature, the pH ranged from about 10–11.3 by adding NaOH to the medium, e.g., 3.1 g NaOH L^{-1} for pH 11.3 medium. The temperature was controlled at 25 °C.

To determine the salinity tolerance profile, the maximum specific growth rates of PNNL-SSL1 were measured at room temperature (ca. 22 °C) at three medium salinities, 10, 15 and 25 PSU. The salinity gradient was generated by varying the amount of NaCl added to the culture media, i.e., 0.5, 5.2, and 14.7 g NaCl L^{-1} for making 10, 15, 25 PSU medium, respectively. The salinity gradient was confirmed by conductivity (Model 30 Conductivity Meter, YSI, Yellow Springs, Ohio, USA).

2.4. Biomass growth in raceway ponds

Duplicate climate simulation raceway ponds were employed to estimate the biomass growth of PNNL-SSL1 under outdoor conditions. The pond system can simulate light and water temperature conditions for algal cultivation at a specific location and season [26]. Based on the temperature tolerance profile determined as described in Section 2.2, PNNL-SSL1 is a warm season strain. Therefore, the outdoor pond conditions on a typical summer day, i.e., July 31st, at Mesa, Arizona, U.S.A. were simulated (Fig. 1). The incident light and water temperature conditions were generated by PNNL's Biomass Assessment Tool based on the average of 30-year's observed meteorological data [27,28]. The light and temperature patterns were repeatedly daily. Throughout the experiment, no concentrated CO_2 was supplied to the culture, and CO_2 in the ambient air was the only carbon source for replenishing the inorganic carbon pool in the culture. Both ponds were operated at 20 cm depth, and distilled water was added each day to make up for the evaporative losses prior to sampling. At each sampling, the pH, salinity, alkalinity and biomass concentration were measured. There were two batch culture runs in this experiment, each started with fresh inoculum and medium at pH close to 10.2 and at the optimal salinity.

2.5. Biomass productivity determination

In this study, biomass concentration was measured in ash-free dry weight (AFDW, g L^{-1}). The AFDW was measured by filtering a known volume of sample onto a pre-weighted Whatman GF/F (0.7 μm pore size) fiber glass filter, drying at 105 °C overnight, and ashing at 540 °C for two hours. AFDW was calculated by dividing the change in filter weight by the sample volume. Because biomass growth in raceway ponds is generally linear [29,30], a linear regression was applied to the AFDW versus time curve, and the slope, which represents the volumetric biomass productivity, was multiplied by the culture depth (20 cm) to obtain the areal biomass productivity, in g m^{-2} day^{-1}.

2.6. Carbon mass balance

Dissolved inorganic carbon (DIC) concentration was calculated by measuring the alkalinity, salinity, pH and water temperature, using published methods. The total alkalinity (A_T), measured by titrating the medium to pH 4.0 with 0.2 N sulfuric acid. Carbonate alkalinity (A_C) was calculated via Eq. 3. Contributions from minor buffering components, i.e., phosphate, boric acid, among others, were negligible relative to the large carbonate alkalinity (ca. 190 meq L^{-1}). [OH^-] was derived from the measured pH and the water autoprotolysis constant (K_W, Eq. 4).

$$A_C = A_T - [OH]^- \tag{3}$$

where A_T is the total alkalinity and A_C is carbonate alkalinity.

$$[OH^-] = 10^{pH-K_W} \tag{4}$$

The equilibrium constants used in the calculations, i.e., K_W and the dissociation constants of carbonic acid (K_1 and K_2), were calculated based on Millero et al., [31] for the measured salinity and water temperature at sampling. The concentration of each carbon species was calculated using Eqs. 5, 6 and 7. The term CO_2^* represents the sum of carbonic acid and aqueous CO_2, and DIC was calculated via Eq. 8.

$$[CO_2^*] = \frac{A_C[H^+]^2}{K_1([H^+] + 2K_2)} \tag{5}$$

$$[HCO_3^-] = \frac{A_C[H^+]}{[H^+] + 2K_2} \tag{6}$$

$$[CO_3^{2-}] = \frac{A_C K_2}{[H^+] + 2K_2} \tag{7}$$

$$DIC = [CO_2^*] + [HCO_3^-] + [CO_3^{2-}] \tag{8}$$

Because atmospheric CO_2 was the only external carbon source, the amount of carbon captured from the air (C_{Air}) for a given time interval was estimated by summing the change in DIC concentration (ΔDIC) and the change in biomass carbon concentration ($\Delta C_{Biomass}$) (Eq. 9). A positive value means a net influx of carbon from the air to medium, and a negative value means a net outflux of carbon from the medium to the air. The ratio of the captured air carbon (C_{Air}) to biomass carbon is indicative of how much air carbon ends up in the biomass. The PNNL-SSL1

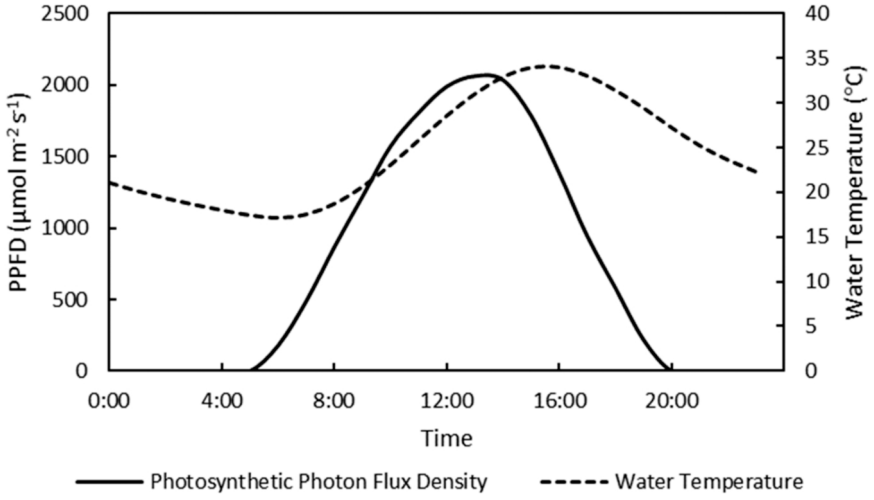

Fig. 1. The scripts of incident light intensity (photosynthetic photo flux density, PPFD, μmol m^{-2} s^{-1}) and water temperature (°C) used in the two batch runs during the climate simulation pond experiment. The script is repeated daily to represent typical outdoor pond conditions in summer at Mesa, Arizona, U.S.A.

pond biomass sample was sent to the Stable Isotope Mass Spectrometry Lab of the Department of Geological Sciences at the University of Florida for carbon content analysis. The result showed that carbon accounts for 53 ± 2% of the AFDW. This value was used to calculate $\Delta C_{Biomass}$ based on daily measured AFDW.

$$C_{Air} = \Delta DIC + \Delta C_{Biomass} \quad (9)$$

where C_{Air} is carbon captured from air, ΔDIC is the change in DIC, and $\Delta C_{Biomass}$ is the change in carbon fixed in biomass.

3. Results and discussion

3.1. Strain identification

The newly isolated strain is a unicellular cyanobacterium, occasionally making small chains of attached oblong cells when dividing rapidly (Fig. 2a). The cell diameter is approximately 3 μm. Phylogenetic analysis indicated that the strain PNNL-SSL1 is most similar to *Cyanobacterium* sp. HL-69 (99% shared identities, Fig. 2b), a cyanobacterium that was recently isolated by scientists at Pacific Northwest National Laboratory (Richland, Washington) from Hot Lake, Washington [32]. PNNL-SSL1 also showed high similarity to *Cyanobacterium stanieri* PCC 7202 (99% shared identities), a strain isolated in an alkaline pond in Chad [33] and the type species for the genus Cyanobacterium [34]. The sequence data of PNNL-SSL1 was submitted to GenBank (accession number: OP933704).

3.2. Temperature tolerance profile

The temperature tolerance profile of *Cyanobacterium sp.* PNNL-SSL1 is shown in Fig. 3. Due to the buffering capacity of the high alkalinity (ca. 190 meq L^{-1}) medium, the culture pH remained relatively stable between 9.4 and 9.9 across the eight temperature levels throughout the experiment. At temperatures of 10 °C or below, no growth was observed. As temperature increases from 10 °C to 40.8 °C, the maximum specific growth rate increased and reach the maximum value of 4.2 day^{-1}. Within the temperature range of 29–40.8 °C, the maximum specific growth rates were not statistically different (p-value > 0.05). No growth was observed above 45 °C. This shape pattern of the thermal response in growth rates from a minimum to a maximum temperature, followed by a sharp drop-off when temperature exceeds the optimum, is observed for many other cyanobacteria and microalgae. For instance, the photosynthesis rate of *Spirulina platensis* was observed to peak at 35 °C and was

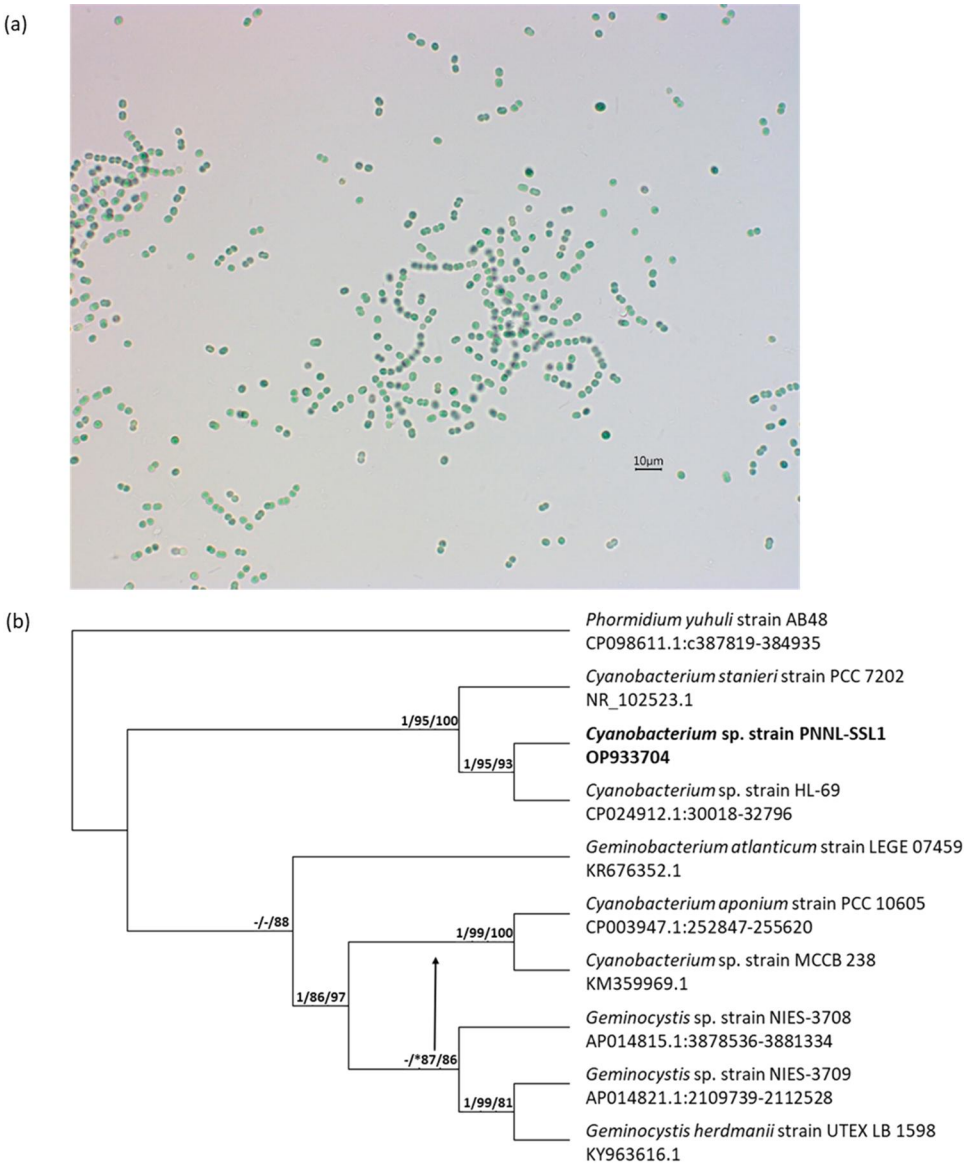

Fig. 2. (a) Microscope image of *Cyanobacterium* sp. PNNL-SSL1; (b) The tree is rooted with *Phormidium yuhuli* strain AB48. The numbers at the nodes are support values for Bayesian posterior probability (BPP), Maximum Likelihood bootstrap (MLBS) and Neighborhood Joining bootstrap (NJBS). Support values of less than 0.9 for BPP, 80 for MLBS, or 80 for NJBS are represented by hyphens. The arrow indicates the alternative position for Geminocystis sp. strain NIES-3709 in the MLBS tree. Genbank accession numbers are shown below the strain names.

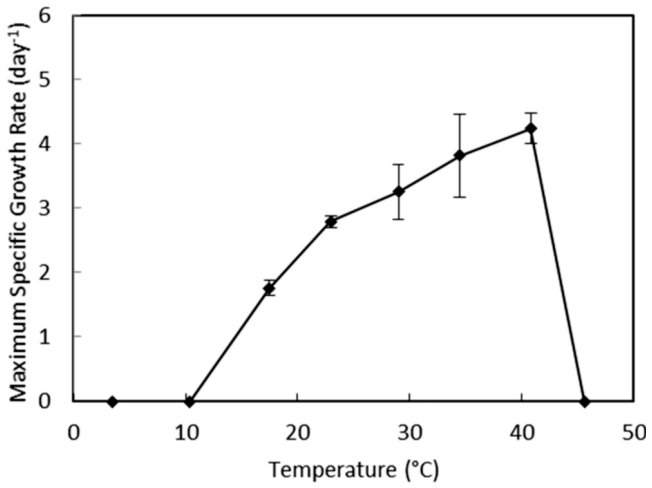

Fig. 3. Average maximum specific growth rate of *Cyanobacterium* sp. PNNL-SSL1 as a function of temperature at pH 11. Error bars represent one standard error (n ≥ 5).

reduced at both lower and higher temperatures [35]. The optimal temperatures of *Synechococcus* and *Prochlorococcus* are 28 °C and 24 °C, respectively, and the growth rates of the two strains decrease as temperature further increases [36]. Based on the result that the maximal specific growth rate was observed at 40.8 °C, PNNL-SSL1 is a warm season strain. Therefore, summer conditions were used for simulating outdoor pond biomass growth in the indoor climate-simulation raceway ponds. As shown in Fig. 1, the water temperature in a 20 cm deep outdoor raceway pond at Mesa, Arizona typically varies from 17° to 34°C in summer season.

3.3. pH tolerance profile

Due to the strong media buffering capacity, relatively thin cultures, and daily dilution with fresh medium, the pH remained relative stable within 0.2 units of target value over the course of the experiment. The highest maximum specific growth rates of PNNL-SSL1 exhibited at pH between 10 and 10.5 (Fig. 4). This result is not surprising because the pH of the isolation location of PNNL-SSL1, Soap Lake, where pH is generally around 10 [37]. For pH above 10.5, the maximum specific growth rate decreased with the increasing pH. At pH 11.3, the highest level tested, PNNL-SSL1 grew at 1.87 day^{-1}, a growth rate greater than observed for

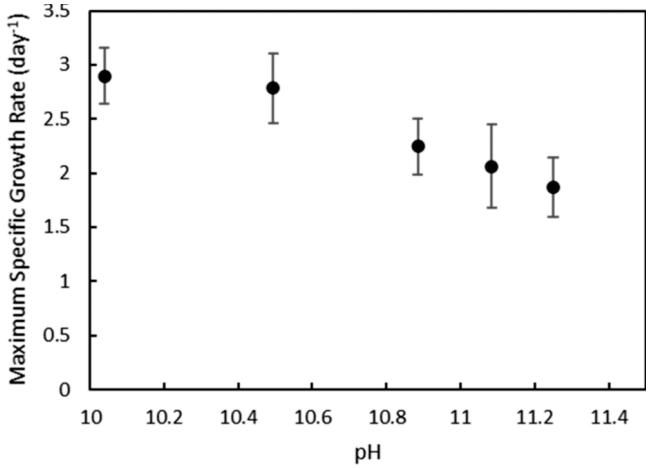

Fig. 4. Average maximum specific growth rate of *Cyanobacterium* sp. PNNL-SSL1 as a function of medium pH. Error bars represent one standard error (n ≥ 6).

many other algae at pH near 10 [38-40], indicating that PNNL-SSL1 is a promising strain for cultivation in the high pH range. Ataeian et al. [11] demonstrated atmospheric CO_2 supported biomass production by growing cyanobacteria consortium between pH 10.4 and 11.2. The excellent specific growth rate of PNNL-SSL1 at pH 11.3 suggested its potential to achieve robust growth while pushing for high atmospheric CO_2 transfer rate.

The decline in the maximum specific growth rate at pH greater than 10.5 is not unexpected as alkaliphilic algae must maintain stable intracellular pH values even at high external pH. *Spirulina platensis* maintains an average intracellular pH of 7.9 at an extracellular pH of 12.2 [41], and *Synechocystis* species can maintain a pH gradient of more than 2 pH units across the membrane at an external pH of 10 [42]. However, the higher the extracellular pH, the greater the challenge that the algal cells face in maintaining cytoplasmic pH homeostasis. Although the elucidation of pH gradients in PNNL-SSL1 cells is beyond the scope of the present study, it is reasonable to assume that the capability of PNNL-SSL1 to balance intracellular pH diminishes as medium pH increases to above 10.5, resulting in declining specific growth rates in the high pH range.

In addition to maintaining a stable intracellular pH, another critical factor in determining the maximum specific growth rate at high pH is the carbon availability. Despite the large amount of carbon in the culture medium, most of the carbon is in the form of carbonate at high pH, which cannot be used by cyanobacteria. PNNL-SSL1, presumably similar to many cyanobacteria and eukaryotic microalgae, has developed carbon concentrating mechanisms (CCM) that accumulate HCO_3^- intracellularly and secure a high CO_2 concentration near RuBisCO to continue photosynthesizing at a low externalHCO_3^- concentration [43-45]. In alkaline medium, dissociation constants of carbonic acid are affected by salinity and temperature. Fig. 5 shows an example of carbon speciation as a function of pH using constants measured by Millero et al., [31] by accounting for the impacts of salinity and temperature. At extremely high pH levels, CO_2 is negligible, and little DIC exists in the form of HCO_3^-. For example, although the medium used in the present study contains 1.4 g L^{-1} DIC, at pH 11.3, HCO_3^- only makes up less than 1% of the DIC. In other words, less than 0.014 g L^{-1} DIC is available to the cells. With such low carbon availability, the intracellular carbon could be limited as the uptake rate of HCO_3^- is dependent on the concentration of the external HCO_3^- [46]. Moreover, carbon transportation via CCM is an energy-demanding process which further increases the penalty on biomass growth at high pH [47]. Therefore, a high carbonate alkalinity

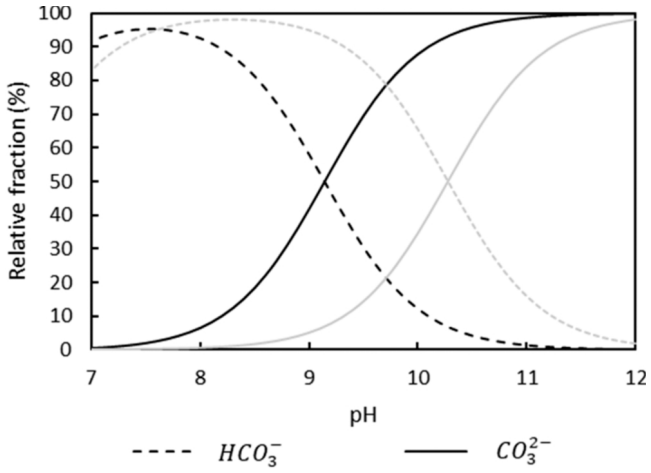

Fig. 5. Relative fraction of bicarbonate and carbonate as a function of pH for the medium used to grow *Cyanobacterium* sp. PNNL-SSL1 (black lines). Dissociation constants of carbonic acid were obtained from Millero et al., [31] for medium at 18.5 PSU and 25 °C. For reference, the gray lines show the relative fraction of bicarbonate and carbonate as a function of pH in freshwater at 20 °C.

is necessary to provide sufficient inorganic carbon, HCO_3^-, to avoid an appreciable growth reduction.

3.4. Salinity tolerance profile

The average maximum specific growth rates at 10, 15, 25 PSU near pH 10 were 3.06 ± 0.25 day^{-1}, 2.77 ± 0.49 day^{-1}, and 2.24 ± 0.1 day^{-1}, respectively (Fig. 6). It is apparent that the increased salinity induces salinity stress and inhibits the growth of PNNL-SSL1. Such inverse correlation between growth and salinity has been reported in other cyanobacteria [48,49]. Some alkaliphilic cyanobacteria, such as *Arthrospira* (*Spirulina*), exhibited declining growth rates and photosynthetic activity as salinity increased [50-52]. Although higher growth rates may be achieved at a lower salinity by reducing the carbonate and bicarbonate salts usage , this strategy was not pursued as a high inorganic carbon concentration in the medium is necessary for supporting algal growth at high pH, as indicated in Fig. 5. However, the dynamics among biomass growth, salinity, carbonate alkalinity and pH change deserve more investigation. For this study, 10 PSU was deemed the optimal salinity for PNNL-SSL1 and was used in the subsequent climate simulation pond experiment.

3.5. Biomass growth in climate simulation ponds

Biomass concentration (g AFDW/L) as a function of time during the raceway pond trial in 10 PSU salinity, 190 meq L^{-1} modified BG11 media is shown in Fig. 7. The biomass concentration is reported as the average of triplicate measurements of AFDW for duplicate pond cultures. The average biomass productivity was 15.2 g m^{-2} day^{-1}, with 15.6 g m^{-2} day^{-1} for the first batch run and 14.8 g m^{-2} day^{-1} for the second batch run, respectively. The biomass productivity of SSL1 observed in the present study agrees with the productivity range reported in previous studies on raceway pond cultivation of cyanobacteria. During *Spirulina* outdoor pond trials in southern Spain, Jiménez et al. [53] reported a peak summer biomass productivity of 13.5 g m^{-2} day^{-1} when cultivated without supplemental CO_2 addition. Vadlamani et al. [12] demonstrated biomass productivity greater than 16 g m^{-2} day^{-1} in absence of CO_2 gas addition using an alkaliphilic green alga, *Chlorella sorokiniana*. Other studies have shown that higher biomass productivity could be achieved by using concentrated CO_2. For instance, Vonshak et al. [54] reported a higher biomass productivity of 22.4 g m^{-2} day^{-1} in the outdoor pond cultivation of *S. platensis* by supplementing the cultures with CO_2 gas. *S. platensis* was reported to reach up to 25 g m^{-2} day^{-1} at higher pond water temperatures [55]. Zhu et al. [13] measured 13.2–18.7 g m^{-2} day^{-1} in *Spirulina* ponds fertilized with industrial flue gas, similar to the biomass productivity achieved by PNNL-SSL1 with direct air CO_2 capture.

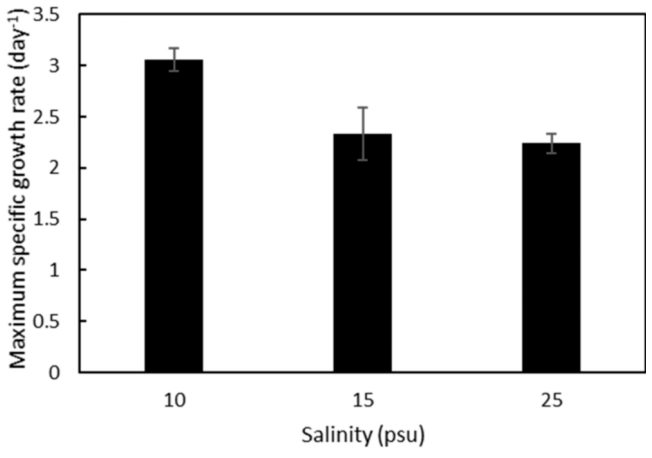

Fig. 6. Average maximum specific growth rate of *Cyanobacterium* sp. PNNL-SSL1 as a function of medium salinity. Error bars represent one standard error (n ≥ 4).

The uptake of nutrients, e.g., HCO_3^- and NO_3^-, results in increased OH^- concentration [56,57]. As a result, the pH in both batch runs increased with time as biomass accumulated, despite the high medium alkalinity (Fig. 7). In the first run, the medium pH increased from 10.17 on day 0 to 10.55 on day 6. In the second run, the medium pH increased from 10.28 on day 11 to 10.71 on day 16. Referring to the growth curves, it is noticeable that the biomass growth slowed down at the end in both runs, i.e., day 5 in the first run and day 14 in the second run. These two days happened to be the first days in the two runs when the pH reached a level above 10.5. This agreed with the pH tolerance profile that the maximum specific growth rate of PNNL-SSL1 was found to decline at pH 10.5 and above. In line with such observation, the biomass productivity was lower in the second run than in the first run as the overall pH was higher in the second run.

3.6. Direct air CO_2 capture

Culture media DIC concentration is mediated by inorganic carbon algal uptake due to photosynthesis, air- CO_2 exchange via the air-water interface, and CO_2 released from cellular respiration and re-absorbed into the media. In both batch culture runs, DIC concentration decreased over time (Fig. 8), indicating that the rate of carbon consumption exceeded the rate of carbon recharge. The result indicated that DIC decreased (ΔDIC) by 0.068 g L^{-1} in the first run and 0.043 g L^{-1} in the second run. Based on the AFDW increase and 53% biomass carbon content, 0.24 g L^{-1} and 0.18 g L^{-1} carbon was incorporated into the biomass ($\Delta C_{Biomass}$) in the respective experimental runs. According to Eq. 9, the total captured air CO_2 carbon (C_{Air}) in the two runs were 0.17 g C L^{-1} and 0.11 g C L^{-1}, respectively. Given that the culture depth was 0.2 m, the areal carbon capture rates were 5.7 g C m^{-2} day^{-1} and 6.2 g C m^{-2} day^{-1}, equivalent to 20.9 g CO_2 m^{-2} day^{-1} and 22.6 g CO_2 m^{-2} day^{-1}, respectively. Although the biomass productivity was lower in the second run, the higher pH resulted in a higher CO_2 capture rate. On average, the direct carbon capture rate was 5.9 g C m^{-2} day^{-1} or 21.6 g CO_2 m^{-2} day^{-1}. This is equivalent to 78.8 ton CO_2 ha^{-1} yr^{-1}, a carbon capture rate much greater than wetlands (4.99 ton CO_2 ha^{-1} yr^{-1}, [58]) and mangroves (average 14.9 ton CO_2 ha^{-1} yr^{-1}, [59]).

The fraction of the carbon assimilated into biomass that originated from the air CO_2 can be estimated by dividing C_{Air} by $\Delta C_{Biomass}$. The results show that 72% and 77% of the carbon in the accumulated biomass was captured from the air in the first and second run, respectively. The higher fraction in the second run was due to the higher pH which resulted in an increased CO_2 mass transfer rate and lower carbon consumption rate caused by the stronger pH stress. On average, direct air CO_2 capture contributed 74% of the carbon incorporated into the biomass, and the remaining 26% was contributed by the inorganic carbon buffering system added during medium preparation. Clearly, the carbon consumption rate of PNNL-SSL1 was greater than the CO_2 in-gassing rate during the linear growth phase where the cultures were growing most actively. To realize 100% air CO_2 supported biomass cultivation, one option is to increase the culture pH to further improve the chemical reaction enhanced CO_2 mass transfer, which, however, requires improved pH tolerance of PNNL-SSL1. The alternative is to identify strains with stronger tolerance to high pH than PNNL-SSL1, such as *Phormidium alkaliphilum*, a recently reported alkaliphilic cyanobacterium that was able to grow at pH up to 11.4 in tubular photobioreactors [60], to enable cultivation at higher pH ranges without severely suppressing growth. It should also be pointed out that, as shown by previous research, both the biomass growth and gas exchange in the algal culture are affected by operational factors such as culture depth and paddlewheel rotation speed [61-63]. Vadlamani et al. [12] demonstrated that the CO_2 in-gassing rate exceeded the carbon consumption by biomass growth during cultivation of *Chlorella sorokiniana*, possibly because the mixing rate was higher in their study, as indicated

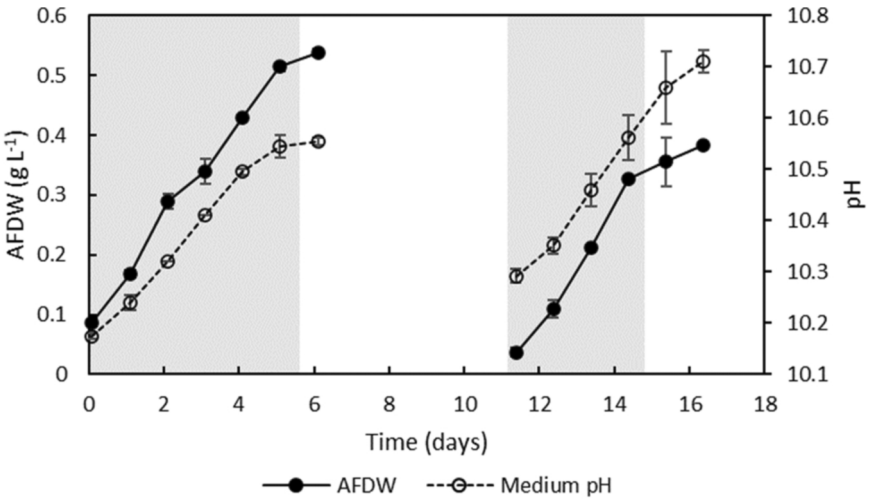

Fig. 7. Average biomass growth (AFDW, g L^{-1}) and pH as a function of time during the climate simulation pond experiment. Error bars represent one standard error (n = 2). Shaded areas indicated the time period for calculating biomass productivity during the linear growth phase.

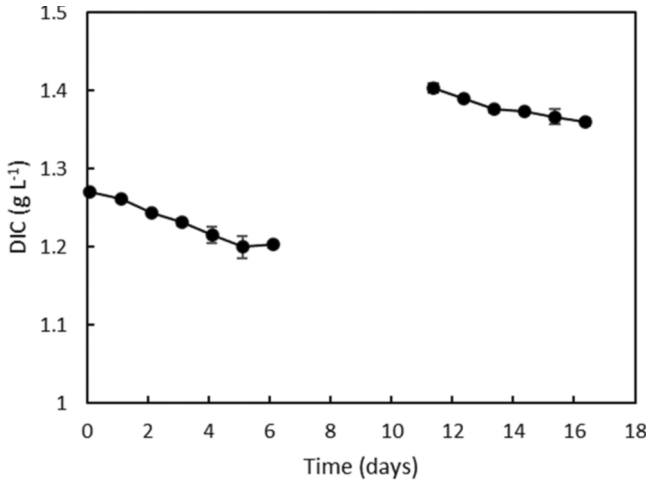

Fig. 8. Change in dissolved inorganic carbon (DIC) concentration during the *Cyanobacterium* sp. PNNL-SSL1 climate-simulation pond culture experiment. Error bars represent standard error (n = 2).

by the higher flow rate of 30 cm s^{-1} versus 11 cm s^{-1} in this study. However, increasing mixing in the pond is likely to result in higher energy cost. Future research could be directed to identifying optimal operational parameters that attain a higher CO_2 mass transfer rate without significantly increase energy cost and exploring technologies that utilize free energy such as wave energy as proposed by Zhu et al. [14].

4. Conclusion

Microalgae cultivation using atmospheric CO_2 can greatly increase the available sites for biomass production and reduce the cost for gas transportation. This work is our first evaluation of the newly isolated alkaliphilic cyanobacterium, *Cyanobacterium* sp. PNNL-SSL1, for biomass cultivation using only air CO_2. The strain showed biomass productivity comparable to previously reported results, and approximately 74% of the photosynthetically assimilated carbon was contributed by directly captured air CO_2. To achieve 100% air CO_2 supported biomass production, future research is necessary to further enhance carbon mass transfer rate without reducing biomass productivity. Although there is space for improvement, this study has demonstrated that PNNL-SSL1 is a promising strain for biomass cultivation using CO_2 from the air.

Data Availability

Data will be made available on request.

Acknowledgement

Pacific Northwest National Laboratory (PNNL) is operated by the Battelle Memorial Institute for the U.S. Department of Energy under contract No. DE-AC05-76RL01830. This research was conducted at PNNL as part of the BETO Incubator project funded by the U.S. Department of Energy (DOE) Office of Energy Efficiency and Renewable Energy (EERE), Bioenergy Technology Office, under Award No. EE0007004. Neither the United States Government nor any agency thereof, nor any of its employees, makes any warranty, express or implied, or assumes any legal liability or responsibility for the accuracy, completeness, or usefulness of any information, apparatus, product, or process disclosed, or represents that its use would not infringe privately owned rights. Reference herein to any specific commercial product, process, or service by trade name, trademark, manufacturer, or otherwise does not necessarily constitute or imply its endorsement, recommendation, or favoring by the United States Government or any agency thereof. The views and opinions of authors expressed herein do not necessarily state or reflect those of the United States Government or any agency thereof.

CRediT authorship contribution statement

Song Gao: Conceptualization, Methodology, Investigation, Formal analysis, Data curation, Visualization, Writing – original draft, Writing – review & editing. **Kyle Pittman:** Investigation, Data curation. **Scott Edmundson:** Supervision, Resources, Writing – review & editing. **Michael Huesemann:** Funding acquisition, Conceptualization, Supervision, Project administration, Writing – review & editing. **Mattias Greer:** Investigation. **William Louie:** Resources. **Peter Chen:** Resources. **David Nobles:** Investigation. **John Benemann:** Conceptualization, Writing – review & editing. **David Noble:** Investigation, Writing – review & editing. **Braden Crowe:** Writing – review & editing.

Declaration of Competing Interest

The authors declare that they have no known competing financial

interests or personal relationships that could have appeared to influence the work reported in this paper.

References

[1] N.S. Diffenbaugh, D. Singh, J.S. Mankin, D.E. Horton, D.L. Swain, D. Touma, A. Charland, Y. Liu, M. Haugen, M. Tsiang, B. Rajaratnam, Quantifying the influence of global warming on unprecedented extreme climate events, Proc. Natl. Acad. Sci. USA 114 (2017) 4881–4886, https://doi.org/10.1073/pnas.1618082114.

[2] Y. Malhi, J. Franklin, N. Seddon, M. Solan, M.G. Turner, C.B. Field, N. Knowlton, Climate change and ecosystems: threats, opportunities and solutions, Philos. Trans. R. Soc. B Biol. Sci. (2020) 375, https://doi.org/10.1098/rstb.2019.0104.

[3] P. Bórawski, A. Bełdycka-Bórawska, E.J. Szymańska, K.J. Jankowski, B. Dubis, J. W. Dunn, Development of renewable energy sources market and biofuels in The European Union, J. Clean. Prod. 228 (2019) 467–484, https://doi.org/10.1016/j.jclepro.2019.04.242.

[4] S.D. Fernandes, N.M. Trautmann, D.G. Streets, C.A. Roden, T.C. Bond, Global biofuel use, 1850-2000, Glob. Biogeochem. Cycles 21 (2007) 1–15, https://doi.org/10.1029/2006GB002836.

[5] J.R. Benemann, I. Woertz, Autotrophic microalgae biomass production: from niche markets to commodities, Ind. Biotechnol. 14 (2018) 3–10, https://doi.org/10.1089/ind.2018.29118.jrb.

[6] L.M.L. Laurens, J. Markham, D.W. Templeton, E.D. Christensen, S. Van Wychen, E. W. Vadelius, M. Chen-Glasser, T. Dong, R. Davis, P.T. Pienkos, Development of algae biorefinery concepts for biofuels and bioproducts; a perspective on process-compatible products and their impact on cost-reduction, Energy Environ. Sci. 10 (2017) 1716–1738, https://doi.org/10.1039/c7ee01306j.

[7] Davis, R., Markham, J., Kinchin, C., Grundl, N., Tan, E.C.D., Humbird, D., 2016. Process Design and Economics for the Production of Algal Biomass: Algal Biomass Production in Open Pond Systems and Processing Through Dewatering for Downstream Conversion. Golden, CO.

[8] M.D. Somers, J.C. Quinn, Sustainability of carbon delivery to an algal biorefinery: a techno-economic and life-cycle assessment, J. CO_2 Util. 30 (2019) 193–204, https://doi.org/10.1016/j.jcou.2019.01.007.

[9] Z. Chi, F. Elloy, Y. Xie, Y. Hu, S. Chen, Selection of microalgae and cyanobacteria strains for bicarbonate-based integrated carbon capture and algae production system, Appl. Biochem. Biotechnol. 172 (2014) 447–457, https://doi.org/10.1007/s12010-013-0515-5.

[10] Z. Chi, Y. Xie, F. Elloy, Y. Zheng, Y. Hu, S. Chen, Bicarbonate-based integrated carbon capture and algae production system with alkalihalophilic cyanobacterium, Bioresour. Technol. 133 (2013) 513–521, https://doi.org/10.1016/j.biortech.2013.01.150.

[11] M. Ataeian, Y. Liu, K.A. Canon-Rubio, M. Nightingale, M. Strous, K. Andrea, C. Rubio, M. Nightingale, Direct capture and conversion of CO_2 from air by growing a cyanobacterial consortium at pH up to 11.2, Biotechnol. Bioeng. 116 (2019) 1604–1611, https://doi.org/10.1002/bit.26974.

[12] A. Vadlamani, B. Pendyala, S. Viamajala, S. Varanasi, High Productivity Cultivation of Microalgae without Concentrated CO_2 Input, ACS Sustain. Chem. Eng. 7 (2019) 1933–1943, https://doi.org/10.1021/acssuschemeng.8b04094.

[13] B. Zhu, H. Shen, Y. Li, Q. Liu, G. Jin, J. Han, Y. Zhao, K. Pan, Large-scale cultivation of *Spirulina* for biological CO_2 mitigation in open raceway ponds using purified CO_2 from a coal chemical flue gas, Front. Bioeng. Biotechnol. 7 (2020) 1–8, https://doi.org/10.3389/fbioe.2019.00441.

[14] C. Zhu, X. Zhai, Y. Xi, J. Wang, F. Kong, Y. Zhao, Z. Chi, Efficient CO_2 capture from the air for high microalgal biomass production by a bicarbonate pool, J. CO_2 Util. 37 (2020) 320–327, https://doi.org/10.1016/j.jcou.2019.12.023.

[15] K. Lívanský, Effect of temperature and pH on absorption of carbon dioxide by a free level of mixed solutions of some buffers, Folia Microbiol. 27 (1982) 55–59, https://doi.org/10.1007/BF02883839.

[16] R. Wanninkhof, M. Knox, Chemical enhancement of CO_2 exchange in natural waters, Limnol. Oceanogr. 41 (1996) 689–697, https://doi.org/10.4319/lo.1996.41.4.0689.

[17] C.Y. Chen, E.G. Durbin, Effects of pH on the growth and carbon uptake of marine phytoplankton, Mar. Ecol. Prog. Ser. 109 (1994) 83–94, https://doi.org/10.3354/meps109083.

[18] J. Mehar, A. Shekh, M.U. Nethravathy, R. Sarada, V.S. Chauhan, S. Mudliar, Automation of pilot-scale open raceway pond: a case study of CO_2-fed pH control on *Spirulina* biomass, protein and phycocyanin production, J. CO_2 Util. 33 (2019) 384–393, https://doi.org/10.1016/j.jcou.2019.07.006.

[19] R. Qiu, S. Gao, P.A. Lopez, K.L. Ogden, Effects of pH on cell growth, lipid production and CO_2 addition of microalgae *Chlorella sorokiniana*, Algal Res. 28 (2017) 192–199, https://doi.org/10.1016/j.algal.2017.11.004.

[20] S. Banerjee, S. Ramaswamy, Comparison of productivity and economic analysis of microalgae cultivation in open raceways and flat panel photobioreactor, Bioresour. Technol. Rep. 8 (2019), 100328, https://doi.org/10.1016/j.biteb.2019.100328.

[21] R. Andersen, Algal Culturing Techniques. Mass, 6th ed.,, Elsevier/Academic Press, Burlington, 2005.

[22] M.W. Fawley, K.P. Fawley, A simple and rapid technique for the isolation of DNA from microalgae, J. Phycol. 40 (2004) 223–225, https://doi.org/10.1111/j.0022-3646.2004.03-081.x.

[23] E.M. del Campo, A. del Hoyo, C. Royo, L.M. Casano, R. Álvarez, E. Barreno, A single primer pair gives a specific ortholog amplicon in a wide range of Cyanobacteria and plastid-bearing organisms: applicability in inventory of reference material from collections and phylogenetic analysis, Mol. Phylogenet. Evol. 57 (2010) 1323–1328, https://doi.org/10.1016/j.ympev.2010.09.014.

[24] S.F. Altschul, W. Gish, W. Miller, E.W. Myers, D.J. Lipman, Basic local alignment search tool, J. Mol. Biol. 215 (1990) 403–410, https://doi.org/10.1016/S0022-2836(05)80360-2.

[25] M. Huesemann, B. Crowe, P. Waller, A. Chavis, S. Hobbs, S. Edmundson, M. Wigmosta, A validated model to predict microalgae growth in outdoor pond cultures subjected to fluctuating light intensities and water temperatures, Algal Res. 13 (2016) 195–206, https://doi.org/10.1016/j.algal.2015.11.008.

[26] M. Huesemann, A. Chavis, S. Edmundson, D. Rye, S. Hobbs, N. Sun, M. Wigmosta, Climate-simulated raceway pond culturing: quantifying the maximum achievable annual biomass productivity of *Chlorella sorokiniana* in the contiguous USA, J. Appl. Phycol. 30 (2018) 287–298, https://doi.org/10.1007/s10811-017-1256-6.

[27] E.R. Venteris, R.L. Skaggs, A.M. Coleman, M.S. Wigmosta, A GIS cost model to assess the availability of freshwater, seawater, and saline groundwater for algal biofuel production in the United States, Environ. Sci. Technol. 47 (2013) 4840–4849.

[28] M.S. Wigmosta, A.M. Coleman, R.J. Skaggs, M.H. Huesemann, L.J. Lane, National microalgae biofuel production potential and resource demand, Water Resour. Res. 47 (2011) 1–13, https://doi.org/10.1029/2010WR009966.

[29] E.W. Becker, Microalgae: Biotechnology and Microbiology, Cambridge University Press, Cambridge, UK, 1994.

[30] E. Lee, M. Jalalizadeh, Q. Zhang, Growth kinetic models for microalgae cultivation: a review, Algal Res. 12 (2015) 497–512, https://doi.org/10.1016/j.algal.2015.10.004.

[31] F.J. Millero, T.B. Graham, F. Huang, H. Bustos-Serrano, D. Pierrot, Dissociation constants of carbonic acid in seawater as a function of salinity and temperature, Mar. Chem. 100 (2006) 80–94, https://doi.org/10.1016/j.marchem.2005.12.001.

[32] J.M. Mobberley, M.F. Romine, J.K. Cole, Y. Maezato, S.R. Lindemann, W.C. Nelson, Draft genome sequence of *Cyanobacterium* sp. Strain HL-69, Isolated from a Benthic Microbial Mat from a Magnesium Sulfate-Dominated Hypersaline Lake, Genome Announc 6 (2018) e01583–17.

[33] R. Rippka, J. Deruelles, J.B. Waterbury, M. Herdman, R.Y. Stanier, Generic assignments, strain histories and properties of pure cultures of cyanobacteria, J. Gen. Microbiol 111 (1979) 1–61, https://doi.org/10.1099/00221287-111-1-1.

[34] R. Rippka, G. Cohen-Bazire, The cyanobacteriales: a legitimate order based on the type strain *Cyanobacterium stanieri*? Ann. l'Institut Pasteur / Microbiol 134 (1983) 21–36, https://doi.org/10.1016/S0769-2609(83)80094-5.

[35] G. Torzillo, A. Vonshak, Effect of light and temperature on the photosynthetic activity of the cyanobacterium *Spirulina platensis*, Biomass Bioenergy 6 (1994) 399–403, https://doi.org/10.1016/0961-9534(94)00076-6.

[36] L.R. Moore, R. Goericke, S.W. Chisholm, Comparative physiology of *Synechococcus* and *Prochlorococcus*: influence of light and temperature on growth, pigments, fluorescence and absorptive properties, Mar. Ecol. Prog. Ser. 116 (1995) 259–276, https://doi.org/10.3354/meps116259.

[37] D.Y. Sorokin, M. Foti, H.C. Pinkart, G. Muyzer, Sulfur-oxidizing bacteria in Soap Lake (Washington State), a meromictic, haloalkaline lake with an unprecedented high sulfide content, Appl. Environ. Microbiol. 73 (2007) 451–455, https://doi.org/10.1128/AEM.02087-06.

[38] J. Piiparinen, D. Barth, N.T. Eriksen, S. Teir, K. Spilling, M.G. Wiebe, Microalgal CO_2 capture at extreme pH values, Algal Res. 32 (2018) 321–328, https://doi.org/10.1016/j.algal.2018.04.021.

[39] D.H. Søgaard, P.J. Hansen, S. Rysgaard, R.N. Glud, Growth limitation of three Arctic sea ice algal species: Effects of salinity, pH, and inorganic carbon availability, Polar Biol. 34 (2011) 1157–1165, https://doi.org/10.1007/s00300-011-0976-3.

[40] K. Spilling, Á. Brynjólfsdóttir, D. Enss, H. Rischer, H.G. Svavarsson, The effect of high pH on structural lipids in diatoms, J. Appl. Phycol. 25 (2013) 1435–1439, https://doi.org/10.1007/s10811-012-9971-5.

[41] S. Belkin, S. Boussiba, Resistance of *Spirulina platensis* to ammonia at High pH values, Plant Cell Physiol. 32 (1991) 953–958.

[42] D.P. Buck, G.D. Smith, Evidence for a Na^+/H^+electrogenic antiporter in an alkaliphilic cyanobacterium *Synechocystis*, FEMS Microbiol. Lett. 128 (1995) 315–320, https://doi.org/10.1016/0378-1097(95)00126-P.

[43] B. Colman, Photosynthetic carbon assimilation and the suppression of photorespiration in the cyanobacteria, Aquat. Bot. 34 (1989) 211–231, https://doi.org/10.1016/0304-3770(89)90057-0.

[44] B.M. Long, B.D. Rae, V. Rolland, B. Förster, G.D. Price, Cyanobacterial CO_2-concentrating mechanism components: function and prospects for plant metabolic engineering, Curr. Opin. Plant Biol. 31 (2016) 1–8, https://doi.org/10.1016/j.pbi.2016.03.002.

[45] G.D. Price, M.R. Badger, F.J. Woodger, B.M. Long, Advances in understanding the cyanobacterial CO_2-concentrating- mechanism (CCM): Functional components, Ci transporters, diversity, genetic regulation and prospects for engineering into plants, J. Exp. Bot. 59 (2008) 1441–1461, https://doi.org/10.1093/jxb/erm112.

[46] D. Sültemeyer, G.D. Price, J.W. Yu, M.R. Badger, Characterisation of carbon dioxide and bicarbonate transport during steady-state photosynthesis in the marine cyanobacterium *Synechococcus* strain PCC7002, Planta 197 (1995) 597–607, https://doi.org/10.1007/BF00191566.

[47] N.M. Mangan, A. Flamholz, R.D. Hood, R. Milo, D.F. Savage, pH determines the energetic efficiency of the cyanobacterial CO_2 concentrating mechanism, PNAS 113 (2016) E5354–E5362, https://doi.org/10.1073/pnas.1525145113.

[48] J.C. Batterton, C. Van Baalen, Growth responses of blue-green algae to sodium chloride concentration, Arch. Mikrobiol. 76 (1971) 151–165, https://doi.org/10.1007/BF00411789.

[49] S. Bemal, A.C. Anil, Effects of salinity on cellular growth and exopolysaccharide production of freshwater *Synechococcus* strain CCAP1405, J. Plankton Res 40 (2018) 46–58, https://doi.org/10.1093/plankt/fbx064.
[50] E. Kebede, Response of *Spirulina platensis* (=*Arthrospira fusiformis*) from Lake Chitu, Ethiopia, to salinity stress from sodium salts, J. Appl. Phycol. 9 (1997) 551–558, https://doi.org/10.1023/A:1007949021786.
[51] A. Vonshak, R. Guy, M. Guy, The response of the filamentous cyanobacterium *Spirulina platensis* to salt stress, Arch. Microbiol. 150 (1988) 417–420, https://doi.org/10.1007/BF00422279.
[52] A. Vonshak, N. Kancharaksa, B. Bunnag, M. Tanticharoen, Role of light and photosynthesis on the acclimation process of the cyanobacterium *Spirulina platensis* to salinity stress, J. Appl. Phycol. 8 (1996) 119–124, https://doi.org/10.1007/BF02186314.
[53] C. Jiménez, B.R. Cossío, F.X. Niell, Relationship between physicochemical variables and productivity in open ponds for the production of *Spirulina*: A predictive model of algal yield, Aquaculture 221 (2003) 331–345, https://doi.org/10.1016/S0044-8486(03)00123-6.
[54] A. Vonshak, S. Laorawat, B. Bunnag, M. Tanticharoen, The effect of light availability on the photosynthetic activity and productivity of outdoor cultures of *Arthrospira platensis* (*Spirulina)*, J. Appl. Phycol. 26 (2014) 1309–1315, https://doi.org/10.1007/s10811-013-0133-1.
[55] A. Richmond, E. Lichtenberg, B. Stahl, A. Vonshak, Quantitative assessment of the major limitations on productivity of *Spirulina platensis* in open raceways, J. Appl. Phycol. 2 (1990) 195–206.
[56] P.G. Brewer, J.C. Goldman, Alkalinity changes generated by phytoplankton growth, Limnol. Oceanogr. 21 (1976) 108–117, https://doi.org/10.4319/lo.1976.21.1.0108.
[57] B. Glaz, Evidence for HCO_3^- transport by the blue-green alga (Cyanobacterium) *Coccochloris peniocystis*, J. Crop Improv 20 (1980) 397–402, https://doi.org/10.1300/J411v20n01_08.
[58] K. Gallant, P. Withey, D. Risk, G.C. van Kooten, L. Spafford, Measurement and economic valuation of carbon sequestration in Nova Scotian wetlands, Ecol. Econ. (2020) 171, https://doi.org/10.1016/j.ecolecon.2020.106619.
[59] D.M. Alongi, Carbon cycling and storage in mangrove forests, Ann. Rev. Mar. Sci. 6 (2014) 195–219, https://doi.org/10.1146/annurev-marine-010213-135020.
[60] M. Haines, A. Vadlamani, W. Daniel Loty Richardson, M. Strous, Pilot-scale outdoor trial of a cyanobacterial consortium at pH 11 in a photobioreactor at high latitude, Bioresour. Technol. 354 (2022), 127173, https://doi.org/10.1016/j.biortech.2022.127173.
[61] M. Caia, O. Bernard, Q. Béchet, Optimizing CO_2 transfer in algal open ponds, Algal Res. 35 (2018) 530–538, https://doi.org/10.1016/j.algal.2018.09.009.
[62] S. Koley, T. Mathimani, S.K. Bagchi, S. Sonkar, N. Mallick, Microalgal biodiesel production at outdoor open and polyhouse raceway pond cultivations: a case study with *Scenedesmus accuminatus* using low-cost farm fertilizer medium, Biomass Bioenergy 120 (2019) 156–165, https://doi.org/10.1016/j.biombioe.2018.11.002.
[63] J.C. Weissman, R.P. Goebel, J.R. Benemann, Photobioreactor design: mixing, carbon utilization, and oxygen accumulation, Biotechnol. Bioeng. 31 (1988) 336–344, https://doi.org/10.1002/bit.260310409.